Coupling Length Scales for Multiscale Atomistics-Continuum Simulations: Atomistically Induced Stress Distributions in Si/Si_3N_4 Nanopixels

Elefterios Lidorikis, Martina E. Bachlechner, Rajiv K. Kalia, Aiichiro Nakano, and Priya Vashishta
Concurrent Computing Laboratory for Materials Simulations, Biological Computation and Visualization Center, Department of Physics & Astronomy and Department of Computer Science, Louisiana State University, Baton Rouge, Louisiana 70803-4001

George Z. Voyiadjis
Advanced Computational Solid Mechanics Laboratory, Department of Civil and Environmental Engineering, Louisiana State University, Baton Rouge, Louisiana 70803
(Received 21 December 2000; published 6 August 2001)

A hybrid molecular-dynamics (MD) and finite-element simulation approach is used to study stress distributions in silicon/silicon-nitride nanopixels. The hybrid approach provides atomistic description near the interface and continuum description deep into the substrate, increasing the accessible length scales and greatly reducing the computational cost. The results of the hybrid simulation are in good agreement with full multimillion-atom MD simulations: atomic structures at the lattice-mismatched interface between amorphous silicon nitride and silicon induce inhomogeneous stress patterns in the substrate that cannot be reproduced by a continuum approach alone.

DOI: 10.1103/PhysRevLett.87.086104 PACS numbers: 68.35.–p, 02.70.Dh, 02.70.Ns, 79.60.Jv

The Semiconductor Industry Association roadmap predicts that semiconductor device feature size will be 70 nm by year 2008. At these small length scales, the high surface-to-volume ratio increases the role of stress inhomogeneities caused by surfaces and interfaces, which may affect the donor distribution by trapping donors in tensile stress regions [1]. Though the experimental resolution to measure stresses and strains has recently reached 100 nm [2,3], tools to investigate stresses and strains for smaller feature sizes still have to be developed. This is an area where computer simulations in conjunction with nanometer scale stress experiments can play an important role [4,5]. For example, intelligent control over growth and etching during nanopixel fabrication can be achieved by simultaneously performing stress and strain simulations.

Traditional computational approaches on larger ($>1\ \mu$m) length scales have treated stresses and strains as a continuum using the finite-element (FE) method [3,6,7] or elastodynamics [8]. A number of continuum mechanics models have also attempted to incorporate a multiscale analysis [9,10]. These approaches, however, are unable to describe certain atomistically induced stresses at the interface of two different materials (especially if one or both are amorphous), where microscopic details of chemical bonding are important.

Multimillion-atom molecular-dynamics (MD) simulations enable the study of these atomistically induced stress phenomena. For example, formation of stress domains in Si nanopixels covered with amorphous Si_3N_4 films was recently [11] observed in MD simulations of 54×36 nm pixels involving 10×10^6 atoms. These stress domains originate from the atomic configuration at the amorphous/crystalline interface and extend throughout the substrate, where the device operates. Unfortunately, the current experimental resolution (>100 nm) to measure stresses is unable to resolve these fine stress patterns (the periodicity of the stress domains is $\sim$10 nm) that are important for sub-100 nm device operations. For intelligent control over these patterns, innovative and integrated experimental/simulations approaches must be developed to bridge the length scale gap between the experimental resolution and the predicted patterns. From the simulation side, one possible approach is to extend the accessible length scale of MD simulations by coupling them with the FE calculation, and thereby providing experimentally observable information [12–17]. Hybrid FE/MD schemes, such as the quasicontinuum method of Tadmor *et al.* [12], the coarse grained molecular-dynamics method of Rudd *et al.* [14], or the concurrent coupling of length scales approach of Abraham *et al.* [17], are equally appropriate for the pixel problem. We have chosen to use the method by Abraham *et al.*

In this Letter, multiscale phenomena in silicon/silicon-nitride nanopixels are studied using the concurrent hybrid FE/MD approach. The detailed atomic structures at the Si/Si_3N_4 interface create inhomogeneous stress patterns that extend throughout the Si substrate. In the crystalline Si_3N_4 case they consist of a parabolic tensile stress well, while in the amorphous Si_3N_4 case they consist of a hexagonal array of stress domains. A detailed comparison between hybrid simulation results and full MD multimillion-atom simulations shows good agreement, validating the hybrid scheme as a cost-effective tool for studying such multiscale phenomena.

Our hybrid scheme simulates a $25 \times 25 \times 1$ nm Si(111) mesa, covered with a $25 \times 25 \times 5$ nm Si_3N_4 film, on a $50 \times 50 \times 15$ nm Si(111) substrate. The lattice mismatch between Si and Si_3N_4 is of the order of 1.2%. The Si_3N_4 film, as well as the Si/Si_3N_4 interface, is treated atomistically with MD while most of the Si

 © 2001 The American Physical Society

substrate is modeled by FE as a continuum; see Fig. 1(a). Periodic boundary conditions are applied on the sides of the substrate, while its bottom is held fixed. We simulate both crystalline (0001) and amorphous Si_3N_4 films.

In the MD region atoms interact with each other through empirical interatomic potentials. For modeling silicon we use the Stillinger-Weber (SW) potential [18], while for Si_3N_4 we use a combination of two- and three-body interaction terms, which include electronic polarizability, charge transfer, and covalent bonding effects [19]. The interaction due to charge transfer is taken to be screened Coulomb potential. A variation of this potential is used for the interactions across the Si/Si_3N_4 interface, in order to account for the correct charge transfer and bonding obtained from first-principles LCAO electronic structure calculations [20].

In the silicon substrate, 20 Å below the Si/Si_3N_4 interface, distortions from equilibrium are relatively small and linear elasticity is sufficient to describe them. In this region, the equations of linear continuum elasticity are solved on a computational grid. The displacement field is discretized on the grid points (nodes), and, within the grid cells (elements), it is interpolated from the nodal values. For this study we use 8-node "brick" elements [we also use 6-node "prism" elements for grid coarsening; see Fig. 1(b)], with linear interpolation for the displacement field. For the constitutive relations we use the elastic constants of silicon as determined from the SW potential. We also use the lumped mass approximation, i.e., the mass is collapsed on the nodes instead of being uniformly distributed. This approximation has been shown to be more appropriate for small atomic-size elements [14].

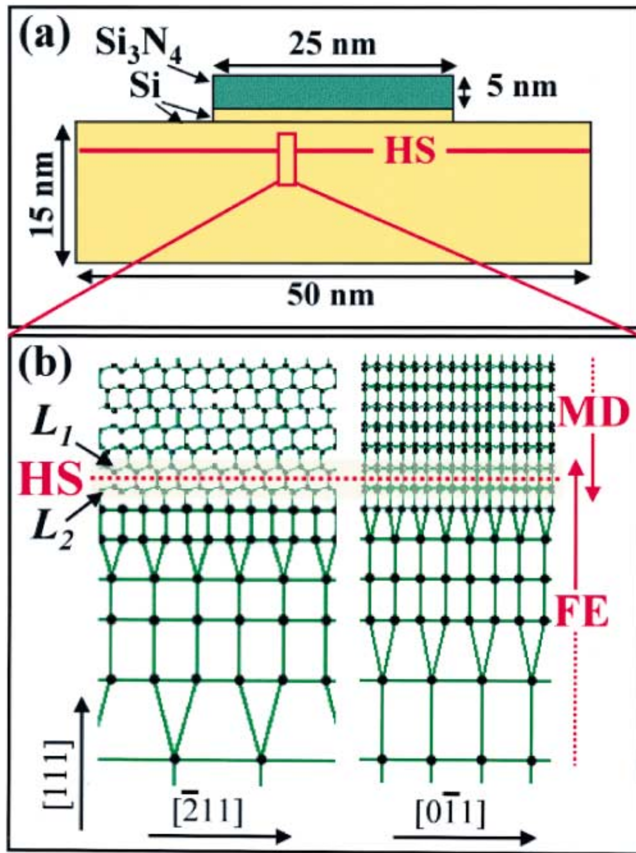

FIG. 1 (color). (a) A schematic of the Si/Si_3N_4 nanopixel. The two dimensional projection shows Si_3N_4 and Si in green and yellow, respectively. Above and below the handshake (HS) region (denoted by the red line), MD and FE apply, respectively. (b) Close-up of the HS region and its surroundings in the Si substrate showing 2D views from two different directions. On the top is the MD region (spheres and lines represent atoms and atomic bonds), and on the bottom is the FE region (spheres and lines represent nodes and element boundaries). The yellow box marks the HS region in which particles are hybrid nodes/atoms, and the red dotted line marks the HS surface.

The MD and FE regions merge seamlessly in the HS region. The FE grid is fine grained down to the atomic scale, and is shifted from the simple cubic arrangement so as to follow the lattice structure of Si. Within the handshake (HS) region the FE and crystalline lattices overlap, yielding a one-to-one correspondence between MD atoms and Fe nodes. For these hybrid atom/node particles we define an "average" Hamiltonian [17] from which their dynamics will follow. The total hybrid Hamiltonian is written as

$$H = \frac{1}{2}\sum_{i}^{N} m_i v_i^2 + \frac{1}{2}\sum_{i,j}^{N_{\text{atoms}}} w_{ij} V_{ij}^{(2)}(\mathbf{r}_{ij}) + \frac{1}{6}\sum_{i,j,k}^{N_{\text{atoms}}} w_{ijk} V_{ijk}^{(3)}(\mathbf{r}_{ij}, \mathbf{r}_{ik}) + \frac{1}{2}\sum_{l}^{N_e}\sum_{i,j}^{N_{ne}} w_l \mathbf{u}_i^l \mathbf{k}_{ij}^l \mathbf{u}_j^l, \tag{1}$$

where N, N_e, and N_{ne} are the number of total particles, elements, and nodes per element, respectively, ($N < N_{\text{atoms}} + N_{\text{nodes}}$ because of the atom/node overlap in the HS). m_i corresponds to both atomic and nodal masses, $V_{ij}^{(2)}$ and $V_{ijk}^{(3)}$ are the two- and three-body potential terms used in MD, and $\mathbf{u}^l$, $\mathbf{k}^l$ are the FE displacement vector and stiffness matrix, respectively, for element l. The SW potential for silicon involves only short range interactions; therefore two bilayers of Si(111) [depicted as L_1 and L_2 in Fig. 1(b)], are sufficient to make up the HS region. By matching the elastic constants of the HS with those of the "bulk" MD and FE systems, we found the following weights in the hybrid scheme to be the most efficient (the three-body weights w_{ijk} are defined similarly to the two-body weights w_{ij}).

$$w_{ij} = \begin{cases} 1 & \text{if } i \text{ or } j \text{ is above } L_1, \\ 3/4 & \text{if } i \text{ and } j \text{ are within } L_1, \\ 1/2 & \text{if } i \text{ or } j \text{ crosses HS}, \\ 1/4 & \text{if } i \text{ and } j \text{ are within } L_2, \\ 0 & \text{if } i \text{ or } j \text{ is below } L_2, \end{cases} \tag{2}$$

$$w_l = \begin{cases} 0 & \text{if } l \text{ is above HS}, \\ 1/2 & \text{if } l \text{ crosses HS}, \\ 1 & \text{if } l \text{ is below HS}. \end{cases}$$

In this way, the potential describing the HS region is approximately weighted as $V \sim (3V_{\mathrm{MD}} + V_{\mathrm{FE}})/4$ for the upper bilayer L_1 and $V \sim (V_{\mathrm{MD}} + 3V_{\mathrm{FE}})/4$ for the lower bilayer L_2.

Our hybrid scheme is computationally highly efficient. Grids in the FE region are generated so that only a small number (10 to 20) of different elements is used [see Fig. 1(b)] which allows us to precalculate and store their stiffness matrices. The time spent on the force computation per simulated node is about 75% of that spent per atom, and so the system size can be enlarged by adding coarsened FE grid with little increase in total computational cost. For example, the computational cost increases only by a factor of 1.5 if FE is used to enlarge the system size by a factor of 4.

The velocity-Verlet algorithm is used for time integration with a time step of $\Delta t = 1$ fs for both MD and FE systems. The combined FE/MD scheme was parallelized through spatial decomposition and run on a 166-node PC cluster at the Concurrent Computing Laboratory for Materials Simulations at LSU.

Our first simulation involves the crystalline Si_3N_4 case. The system is initially relaxed at zero temperature, then heated and thermalized at 300 K using Langevin dynamics, and finally cooled down to zero temperature. In order to achieve a controlled comparison, two systems are prepared, subsequent to the above schedule. In one system, we replace the portion of the substrate below the HS by a FE system, whereas in the other system, the original MD system is kept. Both systems are relaxed according to the same schedule described above.

The comparison between displacement fields of the full MD and the hybrid FE/MD simulations is summarized in Fig. 2. The HS region in the hybrid simulation is only 10 Å below the top of the Si substrate. The absolute displacements from equilibrium $|\Delta r|$ are color coded in Figs. 2(a) and 2(b) for the MD and hybrid systems, respectively. The displacements as a function of the depth z from the top of the pixel, in Fig. 2(c), show very good agreement between the MD and the hybrid schemes.

In Fig. 3 we compare the local stress distributions in the full MD and hybrid FE/MD schemes. The local hydrostatic pressure, i.e., $\sigma = (\sigma_{xx} + \sigma_{yy} + \sigma_{zz})/3$ is color coded in Figs. 3(a) and 3(b) for the MD and hybrid systems, respectively. In Fig. 3(c) we plot the hydrostatic, in-plane and out-of-plane stresses as a function of the depth z. We see the compressive stresses at the top of the Si_3N_4 pixel (due to repulsive forces between the N atoms on the free surface), the compressive stresses just above the interface with Si (Si_3N_4 has a larger lattice constant), the compressive edge stresses at the sides of the Si mesa, and the tensile stress well inside the Si substrate. The hybrid stress curves show two very small "bumps" relative to those of the full MD case. The first is located on the HS region due to the inevitable differences between MD and FE, and the second is in the FE region and is due to the coarsening of the FE grid. Besides these, all features are faithfully reproduced by the hybrid scheme.

To study the effect of the position of the HS region, we perform another FE/MD simulation where the HS is placed 30 Å below the top of the Si substrate instead of 10 Å. Results with two different HS positions are practically identical. This justifies the use of a HS region close to the interface resulting in a highly cost-effective hybrid FE/MD system.

The second simulation we performed is for the Si pixel covered with an amorphous Si_3N_4 film. For this case, it was found that inhomogeneous stress domains are formed

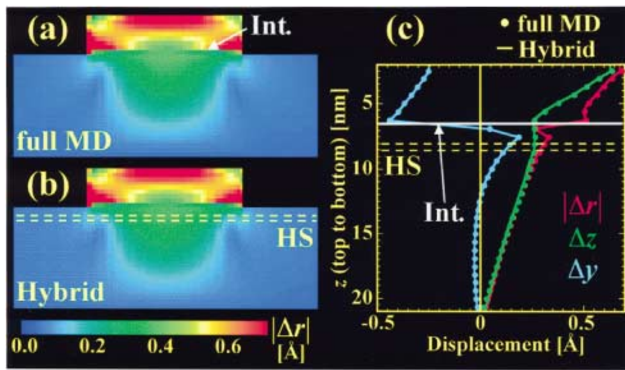

FIG. 2 (color). Absolute displacement from equilibrium $|\Delta r|$ (averaged over a cell) color coded on a slice through the center of the pixel defined by the Si [111] (also denoted as z) and [0-11] (also denoted as y) directions, for (a) the full MD, and (b) the hybrid schemes. In (c), the displacements as a function of the z coordinate (at $x = 0$, $y = d/4$, where $d = 25$ nm is the pixel width and $x = y = 0$ is its center) for both systems are plotted. The Si/Si_3N_4 interface is marked by the horizontal gray line. The HS region for the hybrid system is 10 Å below the top of the Si substrate.

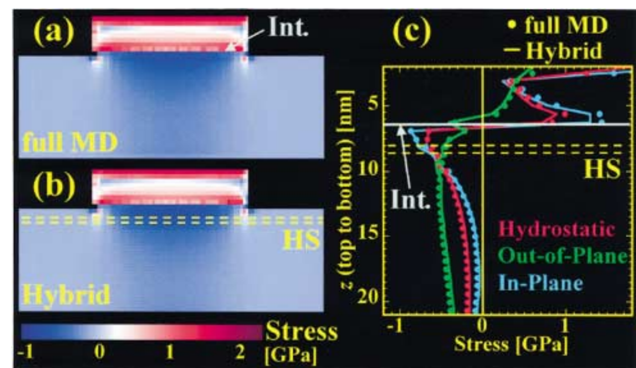

FIG. 3 (color). Hydrostatic stress $\sigma = (\sigma_{xx} + \sigma_{yy} + \sigma_{zz})/3$ for (a) the full MD and (b) hybrid systems, for the same axes as in Figs. 2(a) and 2(b). In (c) we plot the hydrostatic stress, in-plane stress $\sigma = (\sigma_{xx} + \sigma_{yy})/2$, and the out-of-plane stress σ_{zz} as a function of the z coordinate (at the pixel center $x = 0$, $y = 0$) for both systems. The Si/Si_3N_4 interface is marked by the gray line. The HS region for the hybrid system is 10 Å below the top of the Si substrate.

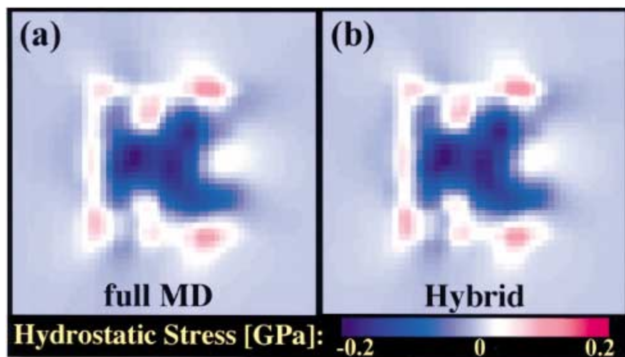

FIG. 4 (color). Stress distribution in the silicon substrate for a silicon nanopixel covered with amorphous Si_3N_4, on a (111) plane 40 Å below the top of the Si substrate for (a) the full MD and (b) hybrid systems. For the hybrid system, this is about 30 Å below the HS region.

below the interface whose shadow can be seen deep into the substrate [11]. The domains are a result of atomistically induced stresses at the lattice-mismatched amorphous/crystalline interface and cannot be observed by a continuum model alone. The size of the domains is determined by the chemistry of the interface and the degree of the lattice mismatch and is of the order of 10 nm. The simulation schedule for amorphous-Si_3N_4-covered nanopixel is the same as the crystalline Si_3N_4 case.

Figure 4 shows stress distributions on a plane parallel to the Si/Si_3N_4 interface and 40 Å below the top of the Si substrate, for the full MD and hybrid schemes. For the hybrid scheme, this corresponds to (30 Å below the HS) deep inside the FE region. The agreement between the two schemes is excellent. All atomistically induced stresses, such as stress domains originating at the interface and edge stresses, are correctly transferred into the continuum. Our hybrid scheme thus successfully couples the two length scales.

In summary, we have applied a hybrid finite-element/molecular-dynamics scheme to study stresses and strains in Si/Si_3N_4 nanopixels. We find a tensile stress well in the crystalline Si_3N_4 case and stress domains in the amorphous Si_3N_4 case, both extending deep into the Si substrate. Excellent agreement is obtained when results are compared with those obtained by using multimillion-atom molecular dynamics. The hybrid FE/MD scheme is validated as a cost-effective method for studying such multiscale phenomena.

This work was supported by the DOE, NSF, AFOSR, and BCVC (Louisiana Board of Regents). Simulations were performed on parallel machines at the Concurrent Computing Laboratory for Materials Simulations.

[1] F. Liu, F. Wu, and M. G. Lagally, Chem. Rev. **97**, 1045 (1997).
[2] S. Di Fonzo *et al.,* Nature (London) **403**, 638 (2000).
[3] Y. Zhuang *et al.,* J. Phys. D **32**, A224 (1999).
[4] Z. Zhang and M. G. Lagally, Phys. Rev. Lett. **72**, 693 (1994).
[5] A. Madhukar, J. Cryst. Growth **163**, 149 (1996).
[6] S. C. Jain *et al.,* J. Appl. Phys. **78**, 1630 (1995).
[7] H. T. Johnson and L. B. Freund, J. Appl. Phys. **81**, 6081 (1997).
[8] P. H. Geubelle and J. R. Rice, J. Mech. Phys. Solids **43**, 1791 (1995); J. W. Morrissey and J. R. Rice, J. Mech. Phys. Solids **46**, 467 (1998).
[9] A. Needleman, Acta Mater. **48**, 105 (2000).
[10] G. Z. Voyiadjis and B. Deliktas, Mech. Res. Commun. **27**, 295 (2000).
[11] M. E. Bachlechner *et al.,* Appl. Phys. Lett. **72**, 1969 (1998); A. Omeltchenko *et al.,* Phys. Rev. Lett. **84**, 318 (2000).
[12] E. B. Tadmor, M. Ortiz, and R. Phillips, Philos. Mag. A **73**, 1529 (1996).
[13] O. A. Shenderova, D. W. Brenner, A. A. Nazarov, A. E. Romanov, and L. H. Yang, Phys. Rev. B **57**, R3181 (1998).
[14] R. E. Rudd and J. Q. Broughton, Phys. Rev. B **58**, R5893 (1998); Phys. Status Solidi (b) **217**, 251 (2000).
[15] M. Mullins and M. A. Dokainish, Philos. Mag. A **46**, 771 (1982).
[16] S. Kohlhoff, P. Gumbsch, and H. F. Fischmeister, Philos. Mag. A **64**, 851 (1991).
[17] F. F. Abraham, J. Q. Broughton, N. Bernstein, and E. Kaxiras, Comput. Phys. **12**, 538 (1998).
[18] F. H. Stillinger and T. A. Weber, Phys. Rev. B **31**, 5262 (1985).
[19] P. Vashishta *et al.,* in *Amorphous Insulators and Semiconductors,* edited by M. F. Thorpe and M. I. Mitkova, NATO ASI, Vol. 23 (Kluwer, Dordrecht, 1997).
[20] G. L. Zhao and M. E. Bachlechner, Phys. Rev. B **58**, 1887 (1998).